Reply to report of reviewer #2
"Errors in satellite-based global horizontal irradiance retrievals due to three-dimensional cloud-radiation interactions by Wiltink et. al."

bold italic font = reviewer's comment
regular font = authors' reply
red regular font = original text in the manuscript
blue regular font = newly added or updated text in the manuscript

---

General remarks

This work assesses the uncertainty in satellite-retrieved global horizontal irradiance (GHI) introduced by the independent pixel approximation (IPA) and plane-parallel approximation (PPA) and the corresponding neglect of 3D radiative effects in current retrievals. In particular, the influence of the spatial resolution on the retrieved GHI is analyzed. To this end, a LES cloud field of shallow cumulus clouds is applied. GHI is retrieved from simulated synthetic TOA reflectance and compared to directly simulated GHI for different scenarios (two solar zenith angles, two surface albedos, two cloud fractions) for varying spatial resolutions. The TOA reflectances as well as the simulated reference GHI are computed using both 1D and 3D radiative transfer solvers. Differences between the retrieved and reference GHIs are explained by the relative importance of irradiance enhancements, shading, and clear-cloudy mixing. In addition, the contributions of the IPA and PPA assumptions to the total bias/RMSE is determined and discussed. The findings highlight the importance to account for 3D radiative effects with increasing spatial resolutions of satellite measurements.

The work addresses an important topic, which is very relevant with higher resolution satellite measurements becoming available, and extends previous work on the influence of 3D radiative effects on cloud and radiation retrievals at different spatial resolutions. However, some additional explanations and further discussions as well as language sharpening/improving would be helpful and should be considered before publication. Please see the general and specific comments below.

We thank the reviewer for taking the time to provide a detailed review of our manuscript. Please find our response to the general and specific remarks below.

In general, it would be very helpful to introduce figures properly and define all variables in the text before referencing them. In particular, please add an explanation on how the effective clearsky, irradiance enhancement, and cloud shadow fractions in Fig. 9 and similar figures were determined and better explain the content of the figures before discussing and analyzing it. This makes it much easier for the reader to follow. More detailed comments are provided below.

We have clarified the use of irradiance enhancement, clear-sky, and cloud shadow fraction by introducing the concepts before discussing the figure's content.

L361. ~~To understand [..] (Fig. 9).~~ → To understand this increase in GHI, we need to consider the balance between irradiance enhanced and shaded pixels. To this end, Figure 9 shows the effective clear-sky fraction (round markers), irradiance enhancement fraction (cross markers) and cloud shadow fraction (square markers). The effective clear-sky fraction is derived from the cloud mask based on the LWP from the LES data. Here the term effective indicates that the fraction of pixels with LWP = 0 kg m^{-2} depends on the spatial resolution, whereas the clear-sky fraction

itself does not. The cloud shadow fraction is computed as the fraction of pixels that are clear-sky and located in the shadow of a cloud, where the shadow calculation is based on a geometrical formula using solar position and the cloud top height, following Wiltink et al. (2025). Finally, the irradiance enhancement fraction is defined as the fraction of pixels for which the 0.64 µm reflectance of the 3D retrieval exceeds that of the 1D retrieval by a predefined threshold, here set to 3 ± 1 %.

The caption of Figure 9 now is as follows:
The effective clear-sky fraction, cloud shadow fraction and irradiance enhancement fraction as a function of spatial resolution. The magnitude of the irradiance enhancement fraction is shown for enhancements of 3% (solid line) and 2 to 4 % (shaded area). The scenarios shown are the same as in Fig. 8.

It is stated that cloudy and clear-sky GHI in the retrieval is computed based on a cloud mask using the liquid water path. However, there is a second cloud mask applying the optical thickness. Why are two different cloud masks used? It is not clear to me, why two different cloud masks are necessary and which cloud mask is exactly used for what. Different cloud masks between the different simulated GHIs and retrievals can affect the results and analyses.
Please see our reply to this point in the specific comment below. Similar concerns were raised by reviewer #1. For further details on cloud masking, please see that reply.

I am missing a discussion about other potential error sources, such as e.g. aerosols, the influence of the cloud morphology, and potential limitations of the presented study. In the study, shallow cumulus clouds were considered and differences between two fields of shallow cumulus clouds with different cloud fractions were demonstrated. I would be careful with too general conclusions due to the limited number of configurations with two solar zenith angles, two cloud fractions, and two surface albedos for a nadir viewing geometry and an additional case for a large viewing zenith angle of 70 degree. The importance of 3D radiative effects is influenced by the complex interaction of the solar and viewing geometry, surface albedo, and cloud fraction with mutual influence. In addition, it strongly depends on the cloud type and the related 3D cloud geometry and microphysics.

We agree with both reviewers that we should be cautious about generalising the results of this study to other cloud types or conditions. Therefore, we have decided to include an additional discussion section focusing on generalisability and error sources (see below).

l. 482 To illustrate the implications [...] in Sect 5.2, results are discussed for two final scenarios in which the retrievals are performed with slanted satellite viewing angles. The discussion section ends with an evaluation of the generalisability and remaining error sources of the conducted simulations (Sect. 5.3).

Generalisability and error sources

The current study remains limited to two variable shallow cumulus cloud fields. Results do not necessarily generalise to other cloud conditions. Likely, in more homogeneous scenes, both IPA and PPA errors will be smaller. Future studies should clarify the influence of 3D cloud-radiation interactions on retrieval accuracy in those conditions.

When generalising the presented results, not only cloud conditions should be considered. As we show in the current study, surface albedo and viewing geometry have a considerable influence on the spatial resolution at which the total bias is minimal. While the minimal total bias of the default scenario of scene 1 occurs at a spatial resolution of 1.6 km, this reduces to 0.4 km (surface albedo = 0.0) or even 0.2 km ($\theta = 40°$) in two of the sensitivity experiments.

Furthermore, in terms of RMSE, at resolutions finer than 2 to 6 km, IPA errors are the most important contributor to the overall error. Also, this balance might shift for other cloud conditions or viewing geometries. For instance, in situations with higher cloud cover and a large optical depth variability, relatively larger PPA contributions might be expected.

Although the different error components may vary strongly across cloud conditions and viewing geometries, the mechanisms describing these errors, as explained in this article, remain valid under these varying conditions, albeit

with a different partitioning. Here, we focused on a single retrieval algorithm (i.e., CPP-SICCS), however, similar results would likely have been found using other 1D physics-based retrieval algorithms.

The scenarios presented in this study have been highly idealised, enabling the illustration of the first-order effect of retrieval errors due to spatial inhomogeneity and 3D radiative transfer effects. Compared to non-synthetic satellite retrievals, some deviations are expected.

For instance, for the current simulations, aerosols were excluded. Although the overall radiative effects of aerosols are much smaller than those of clouds, they still influence GHI. In the presence of aerosols, there will be a stronger extinction of irradiance from the direct beam, especially near cloud edges due to aerosol hygroscopic growth, also leading to increased scattering of radiation into cloud shadows (Gristey et al., 2022). For satellite retrievals, increased scattering would result in stronger irradiance enhancement errors in clear-sky regions. On the other hand, increased scattering towards cloud-shaded regions would reduce the errors related to shadowing.

Furthermore, the current study remains limited to a select number of viewing geometries. These results indicate that biases depend on the viewing geometry. Therefore, the methods of the current study should be extended to other geometries to obtain a more general picture of the effect of viewing geometry on retrieval errors arising from three-dimensional cloud-radiation interactions. In terms of PPA, the transmittance biases plotted in Figure 16 already provide a first indication of the sign and magnitude of this error across a range of viewing geometries.

Furthermore, we have nuanced the statement that, **generally**, biases are minimal at a spatial resolution of 1 to 3 km. We decided to do this because for instance, for the scenario with a surface albedo of 0 and a solar zenith angle of 51°, the total bias is minimal at a spatial resolution of 400 m (Fig. 10b). Moreover, for a new simulation with $\theta = 40°$, (see the reply to reviewer #1), the total bias turns out to be minimal at a spatial resolution of 200 m. The following adjustments will be made for this.

Abstract l.6 This study assesses [..] ~~12.4 km.~~ 12.8 km, for varying surface albedos and viewing geometries.
Abstract. l. 11 ~~Generally~~ In most simulations [. . .].

l. 589 ~~Overall, when the separate bias contributions are added up to the total bias, for simulations with surface albedo of 0.22, the smallest total biases are found at a spatial resolution of around 1 to 3 km, which is in line with findings from previous studies.~~ → For most simulations, when the separate bias contributions are added up, the smallest total biases are found at a spatial resolution of around 1 to 3 km, which is in line with findings from previous studies. However, this does not seem to be a general rule as the sensitivity studies show a strong dependence on surface albedo and satellite and solar geometry. For example, at a viewing zenith angle of 40°, total biases are minimal at a spatial resolution of 0.2 km.

Specific comments

l. 38-39: Strictly speaking, the PPA assumes horizontal homogeneity, vertical variations are accounted for.
That is correct: with the PPA, vertical variations are accounted for. Therfore, the sentence will be adjusted to the following:

l. 38-39 The PPA assumes that all retrieved pixels are ~~fully~~ horizontally homogeneous.

l. 41 and 44: These are very general statements. Maybe add references such as Zinner and Mayer (2006).
We have added the reference to Zinner and Mayer after the statement made in l. 41 and 44.

l. 79: Passive imagers can provide information about 3D cloud geometry. In particular, they can resolve horizontal variations and 3D cloud geometry can, for example, also be derived using stereographic methods.
We believe this comment is related to the statement made in l. 71. We agree that it is more precise here to write sub-pixel variability and vertical cloud structure instead of 3D cloud structure. And indeed, with stereographic methods a 3D cloud field could be reconstructed. This would require observations from different platforms with varying viewing geometries, which is beyond the scope of the current study. We have adjusted the statement made

in line 71 to:

Since measurements from individual passive imagers do not give information on ~~3D~~ sub-pixel variability and vertical cloud structure, it remains impossible from these observations alone to quantify exactly how 3D radiative effects and sub-pixel cloud heterogeneity influence GHI retrievals.

l. 95: Could you add at least one or two sentences about the LES simulations giving just a quick summary about the model and data used for the simulations?
We now mention where the full model setup can be found. Furthermore, we now state the radiative transfer solvers (1D and 3D) used by MicroHH. Finally, a reference to the ERA5 Dataset will be added, which is used as input for the MicroHH simulations.

The LES has been performed using MicroHH (Heerwaarden et al., 2017). The full model setup for the current study can be found in Tijhuis (2024). In MicroHH radiation is solved in 1D using RTE-RRTMPG (Radiative Transfer for Energetics+RRTM for General circulations model applications—Parallel; Pincus et al. (2019)) or in 3D using the raytracer of Veerman et al. (2022) (See section 3.3). The initial and boundary conditions are based on ERA5 (Hersbach et al., 2020) [...].

l. 112-118: You state that you excluded gases besides ozone in your radiative transfer simulations, but the satellite retrieval includes the effects of water vapor and CO2. Why did you not include these gases in the simulations as well to avoid inconsistencies? Later in l. 159 you write that the retrieval does not use other gases. Please clarify.
Currently, for MONKI, the effects of other gases besides ozone have not yet been implemented. Therefore, to be consistent, the CPP retrieval of cloud properties was also performed assuming only absorption by ozone. The subsequent SICCS GHI retrieval does include absorption by water vapour and carbon dioxide, in addition to ozone, and is consistent with the reference simulations based on the LES output. This distinction between the cloud property and GHI retrievals is not fully clear in the paper and therefore we will make the following change in l. 159.

l. 165 As mentioned in Sect. 3.1, the MONKI simulations are fully monochromatic, including only absorption by ozone, and the cloud property retrievals are performed correspondingly.

l. 135: How large is the error introduced by using monochromatic simulations instead of directly simulating the satellite channels by performing simulations for a narrow wavelength band and applying the spectral response function of the channels? I guess the retrieval assumes input reflectances for the real satellite channels in contrast to the simulated monochromatic reflectances.
The CPP retrieval is performed assuming monochromatic reflectances, so this is consistent with the MONKI simulations (see previous comment).

l. 160 + 165: You first mention that you flag pixels as cloudy based on the optical thickness. Besides, you have an additional cloud mask using the liquid water path. Why do you use two different cloud masks and when exactly is which cloud mask applied? Differences between the cloud masks and therefore the classification into cloudy and clear sky affect the GHI estimates and therefore the results and analyses.

We primarily use a cloud mask based on the LWP data from LES. However, the CPP-SICCS retrieval uses it's own internal cloud mask based on reflectance. This internal cloud mask for CPP-SICCS is based on reflectance and is therefore more uncertain. As this study shows the reflectance based cloud mask has limitations regarding 3D radiative effects. Furthermore, errors in surface albedo can also cause errors in the reflectance based cloud mask.

The distinction between both cloud masks will be clarified in the manuscript.

l.121 ~~Finally~~ Furthermore, the cloud droplet effective radii of the scene have been rounded to their nearest integer values, in order to align them to the droplet sizes used in MONKI (see Sect. 3.1). Finally, based on LES data a cloud mask is defined by LWP > 0 kg m^{-2}.

The following paragraph has been removed:

l. 165-168 ~~To distinguish between clear-sky and cloudy pixels a cloud mask is generated based on the liquid water path from the LES data. When the liquid water path for a pixel is larger than 0, the pixel is considered to be cloudy. Note that this cloud mask differs from the retrieved optical depths where also for clear-sky pixels a small non-zero optical depth is possible.~~

Finally, in line 161, the difference between both mask is clarified:

Pixels are flagged as cloudy if the retrieved τ is above zero. Note that this internal retrieval cloud mask differs from the LES based cloud mask.

l. 245: Why is the uncertainty of the retrieved optical thickness larger for optically thicker clouds and the optical thickness increasingly overestimated? For optically thick clouds, the reflectance saturates at some point, which would, however, lead to an underestimation of the optical thickness. Please add a short explanation and a reference.
The relation between visible reflectance and optical thickness is indeed non-linear. At higher reflectances, the corresponding optical depth increases rapidly. Therefore, at high optical thickness, a small uncertainty in reflectance will lead to a large uncertainty in optical thickness. (See Fig. 14 of the study of (Platnick et al., 2017))

Regarding the over- or underestimation of retrieved optical thickness we would like to refer to Figure 2 from Nakajima and King (1990) as an illustration. Assume a visible reflectance of 0.7 with an uncertainty of 0.1 then the retrieval will yield:

- Reflectance 0.7 $\rightarrow \tau \approx 32$
- Reflectance 0.6 $\rightarrow \tau \approx 24$ [-8]
- Reflectance 0.8 $\rightarrow \tau \approx 48$ [+16]

The uncertainty in reflectance leads to a mean overestimation of optical thickness.

To clarify this point, the Reference to Platnick 2017 will be added to the manuscript:

This illustrates the increased absolute uncertainty in the τ retrieval for optically thick pixels (Platnick et al., 2017).

l. 250: How did you decide to use a decay scale of 10? The vertical weighting function generally depends on the vertical cloud structure and solar geometry. Did you compute the weighting functions following Platnick (2000)?
We did not compute weighting functions for the specific conditions, but roughly estimated an exponential decay scale from Figure 5a in Platnick (2000). We performed a quick sensitivity study to assess the influence of the vertical weighing on the presented results. For four different values of τ_w, the effective radius retrieval bias for scene 1 and scene 2 is as follows (bias for pixels with $\tau > 3$ between brackets):

- $\tau_w = 1$: 1.61 and 0.50 µm (1.13 and 0.23 µm)
- $\tau_w = 5$: 1.17 and 0.20 µm (0.53 and -0.17 µm)
- $\tau_w = 10$: 1.17 and 0.27 µm (0.53 and -0.09 µm)
- $\tau_w = 15$: 1.20 and 0.31 µm (0.56 and -0.03 µm)

l. 251: Related to the previous point: deviations of the assumed vertical weighting function from the actual one are an additional explanation for the observed differences between the retrieved and the model values.
The vertical weighing is indeed an additional uncertainty in the validation of the effective radii. Since the vertical weighing has only been applied to validate the effective radii simulated with CPP-SICCS against the one from the LES input, it does not play a role in the further analysis presented in the preprint.

l. 306-308: The probability density functions or the average GHIs become much more similar between the different cases at coarser resolutions, but to be honest the spatial distribution to me looks

very different. They all appear kind of noisy but the structures and the absolute values look very different.
Especially for the comparison between the 1D retrieval and 1D reference spatial patterns remain comparable towards lower spatial resolutions. We agree that compared to the spatial patterns of the 3D reference deviations remain larger. We will now formulated the statement differently:

l. 308: Despite the large local differences [..] are smoothed out, and deviations between the 3D and 1D retrievals and reference become less extreme. ~~3D and 1D retrievals and reference converge towards more comparable GHI fields.~~

Fig. 7 and similar figures: This and similar figures are stated to show the probability density function (PDF), but values up to 400 are observed? Are these then absolute frequency values? Please check and clarify.
Yes, these are PDF's, but because the bin sizes of the PDF's are (much) smaller than 1, this allows the probability densities to exceed 1.The total surface area of the PDF still remains 1.

Fig. 8: Could you add the standard deviations to this and similar plots to also visualize the variability?
Adding standard deviations is possible, however, at the finest resolution, the distributions of the 3D reference and retrieval are bimodal. This means that the standard deviation is considerable. For the finest resolution of the default scenario of scene 1 the standard deviation is 0.39 for the 3D reference. Adding standard deviations to these plots, in our opinion, would not lead to further clarification (See added example).

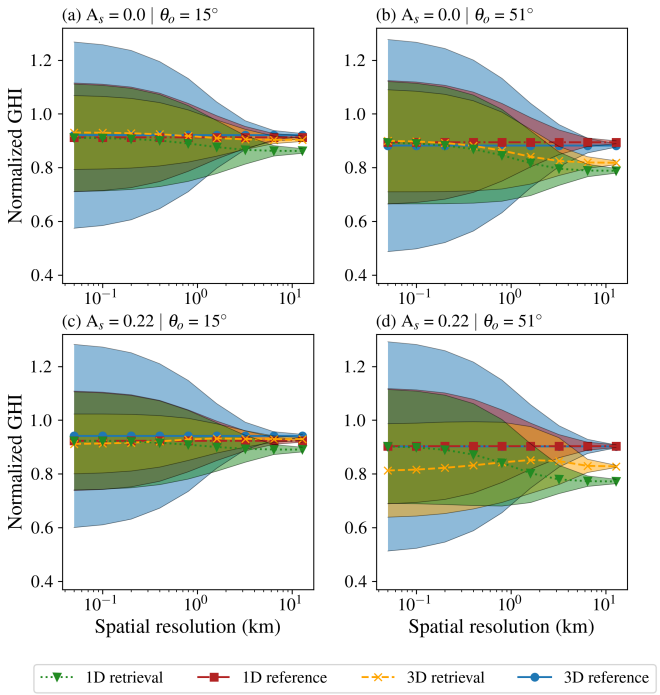

Suggestion 2: Same as Figure 8 in the preprint but now with shaded areas indicating GHI standard deviation

l. 361 / Fig. 9: Please shortly introduce the content of Fig. 9 in the text before using it for the discussion of the results. In particular, please explain how the effective clear-sky fraction, irradiance enhancement fraction and cloud shadow fraction were determined and are defined. These quantities have not been introduced.
See the response to this comment in our reply to the general remarks.

l. 370: Where does the clear-sky reflectance threshold of 0.22 come from?

The explanation presented at l. 370 in the manuscript is based on an older version of the cloud shadow fraction computation, which used reflectance thresholds. The results are very similar to those of the current method, but the presented explanation is not correct.

In our current method, the cloud shadow fraction is defined as the fraction of pixels that are clear-sky and shaded. Whether a pixel is clear-sky or cloudy is determined by the LES cloud mask (and not by reflectance). Shadow pixels are computed using a geometric formula that uses the solar position and cloud-top height. Consequently, the cloud shadow fraction is independent of reflectance. This is will be explained in the beginning of the section (see response to the general remarks of this review) and therefore we will remove the lines 367 – 370.

l. 367 – 371: Meanwhile, it is shown that the cloud shadow fraction (square markers in Fig. 9d) remains constant until a spatial resolution of about 0.8 km ~~The explanation for this is as follows. Cloud shadows are identified as the pixels where the reflectance is below the clear-sky reflectance. Towards coarser spatial resolutions the reflectance of the cloud-shaded pixels gradually increases as mixing with cloudy pixels takes place. But as long as the clear-sky reflectance threshold (in this case 0.22, i.e. the surface albedo) is not exceeded, shadows remain~~, and so does the retrieval error due to shading.

l. 377-385: The solar zenith angle also affects the magnitude of the radiation enhancement not only the number of pixels that are affected. The enhancements are related to radiation escaping through and being reflected on the cloud sides whose orientation relative to the sun matters.

The reviewer correctly points out that the magnitude of the irradiance enhancement is also affected by the solar zenith angle. This information is contained in Figure 9, albeit somewhat indirectly. To get an indication of the magnitude of irradiance enhancements for various scenes, one can consider the ratio between the enhancement fractions.

To illustrate, take the enhancement fractions of 3 and 4 % for the scene with $\theta_0 = 51°$ and a surface albedo of 22 %. About 45 % of pixels have an enhancement larger than 3%, and about 15 % of the pixels have an enhancement above 4 %. This means that 33 % of the pixels with an enhancement above 3% also has an enhancement larger than 4%. A similar comparison can be done for the scene with $\theta_0 = 15°$ and a surface albedo of 22 %. For this scene, the irradiance enhancement fractions are exceeding 3 % and 4 % for about 20 % and 1 % of the pixels, respectively. This means that only 5% of all the pixels with an irradiance enhancement exceeding 3 % also exceed 4 %.

Hence, the distributions of the irradiance enhancement magnitudes differ between the two scenarios. For the high sun scenario, there are relatively much fewer pixels with an enhancement exceeding 4%.

To clarify further, l. 379 will be adjusted to:

l. 379 First, both the irradiance enhancement fraction and magnitude at a θ_0 of 15° is smaller than at a θ_0 of 51° (compare cross markers and shaded areas between Fig. 9c and d). Information on the magnitude of irradiance enhancement can be derived from Fig. 9 by comparing the ratios of irradiance enhancement fractions, for instance, those of 3% and 4%. Relatively, there are much fewer pixels with enhancements exceeding 4% for the high sun scenario than for the low sun scenario. Consequently, at a θ_0 of 15° the corresponding retrieval error is smaller than at a θ_0 of 51° and ~~Hence,~~ the 0.05 km GHI is much closer to the reference.

l. 390: Why are irradiance enhancements absent for a surface albedo of 0? Radiation can still be reflected on the cloud sides or escape through them

We attribute the lack of irradiance enhancements in these scenarios to the absence of albedo enhancement, a mechanism described by Mol and van Heerwaarden (2025). We summarise the effects in lines 326-334 of the preprint. In short, with a surface albedo of 0, every photon that hits the surface is absorbed and does not contribute to irradiance enhancement. The reviewer is correct in pointing out that irradiance enhancements remain possible for photons that do not hit the surface. For the current scenes, this contribution is small but not 0. Since the y-axis of Figure 9 ranges from 0 to 80 %, the small contribution of irradiance enhancement originating from cloud sides is not visible. Therefore, we write that irradiance enhancement is practically absent in scenarios with a surface albedo of 0 %.

Fig. 10/14a: Could you add a horizontal line at 0 to make it easier to distinguish between negative and positive biases

Horizontal lines at y=0 will be added.

Fig. 10 /l. 400-408: In the introduction you stated that the validity of the IPA decreases with increasing spatial resolution. So, I would expect that the error due to the IPA also increases with increasing spatial resolution, but the biases related to the IPA in Fig. 10 appear constant and independent of the resolution.

In this study, the IPA error is defined as the GHI obtained from the 1D reference minus the GHI of the 3D reference. If we average GHI towards coarser spatial resolutions, the domain-averaged GHI remains constant both for the 1D and 3D reference. Hence, the IPA bias remains unchanged. However, the IPA RMSE increases rapidly towards finer spatial scales. Thus, the statement that the IPA validity decreases towards finer spatial resolutions is valid when the RMSE is considered.

l. 411: The error due to the PPA increases towards coarser resolution, in agreement with Zinner and Mayer (2006). Add this reference there.
We will add the reference in the following way:
l. 412 Therefore, the observed PPA [...] mixing in the 1D retrieval. The observation that the error due to PPA increases towards coarser spatial resolutions is in line with previous findings by Zinner and Mayer (2006).

l. 423: The impact of 3D radiative effects might be smaller due to the partial compensation, but it is still not irrelevant. Even for the domain averages large biases remain.
We agree with the reviewer that 3D radiative effects are not irrelevant. Therefore, we will reformulate the statement to the following:

l. 423: ~~Because there is to a large degree a cancellation of the IPA bias due 3D radiative effects such as irradiance enhancement and shading, one might come to the conclusion that 3D radiative effects are irrelevant. While this might be true for the domain averaged bias, locally 3D radiative effects strongly influence the errors as is shown by the RMSE in Fig. 11.~~ → Although the IPA bias turns out to be rather small due to counteracting 3D radiative effects such as irradiance enhancement and shading, 3D radiative effects strongly influence local GHI errors as shown by the RMSE in Fig. 11.

l. 430: Is there a simple explanation, why the residual RMSE is less sensitive to the spatial resolution than the other RMSE components?
Unfortunately, we do not have a simple explanation for this behaviour of the residual RMSE. We decided not to go into detail, as the current reasoning (presented below) remains somewhat speculative.

At fine spatial resolution, the residual RMSE can be strongly influenced by retrieval errors due to irradiance enhancement and shadowing, as manifested in differences between TOA-simulated 3D and 1D reflectances. Towards coarser spatial resolutions these errors gradually disappear. As a result, a decrease in RMSE would be expected. Meanwhile, towards coarser spatial resolution, clear-cloudy mixing errors will increasingly contribute to the RMSE. Clear-cloudy mixing occurs for both 1D and 3D retrievals. However, differences in retrieved τ between 1D and 3D retrievals can lead to clear-cloudy mixing differences that contribute to the residual RMSE. We expect that compensation between these errors will lead to a relatively insensitive residual RMSE as spatial resolution decreases.

l. 470: What do the given percentages refer to? How were they computed?
The reviewer is likely referring to the percentages mentioned in l. 460 and shown, for instance, in Fig. 9. If this is the case, we attempted to clarify this by better introducing Fig. 9 (see the response to the general remarks). In short:

- Effective clear sky fraction: The fraction of clear sky pixels at various spatial resolutions computed using the LWP data of the LES simulation
- Cloud shadow fraction: The fraction of pixels that are clear-sky and shaded. Computed from the cloud top height and the solar geometry following the method of Wiltink et al. (2025).
- Irradiance enhancement fraction: The fraction of pixels where the ratio of the 3D reflectance to the 1D reflectance exceeds a predefined threshold (in Fig. 9 defined between 1.02 and 1.04 (i.e. 2 to 4 % relative difference)).

Fig. 13a: Was the behavior of the PDFs for decreasing resolutions similar to scene 1 in Fig. 7? Yes, despite not being shown in Fig. 13 and Fig. 17, the PDFs gradually converge towards more comparable distributions as the spatial resolution gets coarser.

Sect. 5.1 / Fig. 15: This section was very hard to follow, partly because Fig. 15 and the related methods were not introduced properly. I strongly recommend to rewrite and restructure this section. You could first start with the basic idea: apply the retrieval and average results and compare this to the averaged true values, due to non-linearities you expect differences, and properly explain Fig. 15. To me, it was very unclear at the beginning, what you are explaining and why. The figure caption of Fig. 15 contains new methods and many details which should better be included in the text. Why are geometries close to default used and not the exact default geometries? Please also explain the differences between the different columns and what the dashed lines denote in the figure caption. Section 5.1 is one of the more technical passages of the current preprint. Based on the reviewer's comments above, we have tried to clarify this section.

l. 479: ~~To this end [...] errors due to inhomogeneity.~~ → First, in Sect. 5.1, it is explained in further detail how the averaging of reflectances from adjacent clear and cloudy pixels can introduce errors in the retrieval. Then, to illustrate the [...]

Clear and cloudy sky mixing errors

l. 484-502: To illustrate how clear-cloudy mixing can introduce transmittance biases in the retrieval via reflectance averaging, we assume a new, highly idealised cloud field consisting of just two pixels in this section. The first pixel has a very low optical depth of 0.25, and the other pixel has a τ of either 5, 25 or 90. The satellite and solar geometry of this idealised scenario are taken directly from the DAK LUT (see section 3.2) and closely match the default used in this study (Table 1).

In Figure 15, for the chosen geometry, the relation between reflectance (solid blue curves) and optical depth as well as transmittance (dash dotted green curves) and optical depth are presented for the three optical depth contrasts between $\tau = 0.25$ and $\tau = 5$ (Fig. 15a and d), $\tau = 25$ (Fig. 15b and e) or $\tau = 90$ (Fig. 15c and f), respectively. In Figs. 15a,b,c the narrowband TOA reflectance at 0.64 µm is plotted, while in Figs. 15d,e,f the (hemispheric) broadband TOA albedo is shown.

The relation between τ and reflectance is highly nonlinear, as demonstrated by the solid, blue curves in Figure 15. As a result, coarsening of the the spatial resolution by averaging the retrieved reflectances of the two pixels (indicated by the open blue circles on the reflectance curves), leads to a substantially lower τ than would have been obtained if, instead of reflectances, the optical depth of both pixels would have been averaged (indicated by the crosses on the dashed lines between the reflectance curves).

With the optical depth determined, the next step is to derive surface irradiance. For this, the relation between τ and transmittance is used (indicated by the green dashed-dotted curves). This relation is also highly nonlinear, causing another inhomogeneity error. However, when the narrowband TOA albedo is used to retrieve τ, the relation between transmittance and optical depth is almost exactly the inverse of that between τ and TOA albedo (Figs. 15d,e,f). Hence, if broadband TOA albedo observations are used to retrieve τ and subsequently transmittance, the respective errors cancel out (see also Greuell et al., 2013): the retrieved transmittance for the combined pixel (indicated by the open green circles on the transmittance curves) is very close to the average of the retrieved transmittance for the individual pixels (indicated by the green crosses on the the dotted lines between the transmittance curves).

However, the current study does not use broadband (hemispheric) TOA albedo to derive τ but rather narrowband TOA reflectances, corresponding to measurements from satellite imagers. For these non-hemispheric observations, the relation with τ (solid lines in Figs. 15a,b,c) is slightly different from that for the broadband TOA albedo (solid lines in Figs. 15d,e,f). As a result, depending on the geometry, the τ retrieval offset is not fully compensated for by the transmittance retrieval. Indeed, the retrieved transmittance at coarse resolution (open green circles in Figs. 15a,b,c) is lower than the actual value (green crosses). Notably, if the clear-cloudy contrast grows, the magnitude

of this negative transmittance bias grows accordingly, as indicated by the larger deviation between the horizontal, yellow, dashed lines. [...]

l. 593/594: This is a very general statement. Your study is based on a limited number of configurations for a specific cloud type, namely shallow cumulus clouds. For the analyzed small number of cases, the conclusion is justified, but you should be careful with generalizations. For stratiform clouds, current GHI retrievals might still perform sufficiently well at higher spatial resolutions. In addition, the influence of solar and viewing geometry, surface albedo, cloud fraction, cloud geometry etc. is very complex and cannot easily be separated. You provided a valuable first investigation of different influencing factors, but for a complete picture much more cloud cases and different solar and viewing geometries etc. would have to be analyzed. In addition, aerosol and other factors, which were not accounted for in your study, could also influence the retrieved GHI. Please add a more detailed discussion about this and the limitations of your work.

We agree with the reviewer's comment and have decided to include an additional discussion section. For further details, please see our response under the general comments section.

Technical corrections:

l. 96: add "horizontal" to resolution
The technical correction will be implemented

l. 97: "with a 25 m resolution" → with a resolution of 25m
The technical correction will be implemented.

l. 127: "create synthetic satellite retrievals"→ create synthetic data for satellite retrievals.
The technical correction will be implemented.

l. 152: "which would additional uncertainties" → which would introduce additional uncertainties
The technical correction will be implemented.

l. 172: "which is the mid-latitude summer value" → which is a typical value for the mid-latitudes in summer?
The technical correction will be implemented.

l. 202: assuming independent and homogeneous pixels? 1D means both applying the IPA and PPA.
For the 1D retrieval and reference indeed the IPA and PPA are applied.

l. 207: In abstract and conclusion the coarsest resolution is 12.4 km, whereas here it is 12.2 km.
The correct coarsest spatial resolution actually is 12.8 km. (Also see our reply to reviewer # 1.) This will be corrected in all instances.

l. 238: eliminate the last "resolution".
The technical correction will be implemented.

l. 258: "in 4" → "in Fig. 4".
The technical correction will be implemented.

l. 285: the top 2 rows of Fig 6 show 1D retrieval and 1D reference but you refer to 3D reference and 1D (reference?) GHI fields.
With this sentence the aim is to compare the 1D retrieval against the 3D reference and compare the 1D reference against the 3D reference. To clarify, the sentence will be adjusted.

l.286 At the finest spatial resolutions, there are distinct differences between the 3D reference and the 1D retrieval and reference GHI fields (top 2 rows of Fig. 6).

l. 355: geometry → solar geometry
The technical correction will be implemented.

l. 386: cross and triangular markers?
The statement in l. 386 is indeed true both for the 1D retrieval (triangular markers) and the 3D retrieval (cross markers). The technical correction will be implemented.

l. 502: add: . . . between the horizontal, yellow dashed lines in the middle and right columns.
The technical correction will be implemented.

Fig. 17b: These values are again normalized by clear-sky GHI?
These values have indeed been normalised by the clear-sky GHI.

l. 540: "retrieval 17b" → "retrieval in Fig. 17b"
The technical correction will be implemented.

l. 589: Start a new sentence: . . . total bias. For. . .
The technical correction will be implemented.

In general, I can recommend using Grammarly or similar tools for improving punctuation etc
Grammarly will be used to improve punctuation.

References

Greuell, W., Meirink, J. F., and Wang, P.: Retrieval and validation of global, direct, and diffuse irradiance derived from SEVIRI satellite observations, Journal of Geophysical Research Atmospheres, 118, 2340–2361, https://doi.org/10.1002/jgrd.50194, 2013.

Gristey, J. J., Feingold, G., Schmidt, K. S., and Chen, H.: Influence of Aerosol Embedded in Shallow Cumulus Cloud Fields on the Surface Solar Irradiance, Journal of Geophysical Research: Atmospheres, 127, e2022JD036 822, https://doi.org/10.1029/2022JD036822, 2022.

Heerwaarden, C. C. V., Stratum, B. J. V., Heus, T., Gibbs, J. A., Fedorovich, E., and Mellado, J. P.: MicroHH 1.0: A computational fluid dynamics code for direct numerical simulation and large-eddy simulation of atmospheric boundary layer flows, Geoscientific Model Development, 10, 3145–3165, https://doi.org/10.5194/GMD-10-3145-2017, 2017.

Hersbach, H., Bell, B., Berrisford, P., Hirahara, S., Horányi, A., Muñoz-Sabater, J., Nicolas, J., Peubey, C., Radu, R., Schepers, D., Simmons, A., Soci, C., Abdalla, S., Abellan, X., Balsamo, G., Bechtold, P., Biavati, G., Bidlot, J., Bonavita, M., De Chiara, G., Dahlgren, P., Dee, D., Diamantakis, M., Dragani, R., Flemming, J., Forbes, R., Fuentes, M., Geer, A., Haimberger, L., Healy, S., Hogan, R. J., Hólm, E., Janisková, M., Keeley, S., Laloyaux, P., Lopez, P., Lupu, C., Radnoti, G., de Rosnay, P., Rozum, I., Vamborg, F., Villaume, S., and Thépaut, J.-N.: The ERA5 global reanalysis, Quarterly Journal of the Royal Meteorological Society, 146, 1999–2049, https://doi.org/10.1002/qj.3803, 2020.

Mol, W. and van Heerwaarden, C.: Mechanisms of surface solar irradiance variability under broken clouds, Atmospheric Chemistry and Physics, 25, 4419–4441, https://doi.org/10.5194/ACP-25-4419-2025, 2025.

Nakajima, T. and King, M. D.: Determination of the Optical Thickness and Effective Particle Radius of Clouds from Reflected Solar Radiation Measurements. Part I: Theory, JOURNAL OF THE ATMCBPHERIC SCIENCES, 47, https://doi.org/10.1175/1520-0469(1990)047\%3C1878:DOTOTA\%3E2.0.CO;2, 1990.

Pincus, R., Mlawer, E. J., and Delamere, J. S.: Balancing Accuracy, Efficiency, and Flexibility in Radiation Calculations for Dynamical Models, Journal of Advances in Modeling Earth Systems, 11, 3074–3089, https://doi.org/10.1029/2019MS001621, 2019.

Platnick, S.: Vertical photon transport in cloud remote sensing problems, Journal of Geophysical Research Atmospheres, 105, 22 919–22 935, https://doi.org/10.1029/2000JD900333, 2000.

Platnick, S., Meyer, K. G., King, M. D., Wind, G., Amarasinghe, N., Marchant, B., Arnold, G. T., Zhang, Z., Hubanks, P. A., Holz, R. E., et al.: The MODIS cloud optical and microphysical products: Collection 6 updates and examples from Terra and Aqua, IEEE Transactions on Geoscience and Remote Sensing, 55, 502–525, 2017.

Tijhuis, M.: Code used for publication about coupled 3D radiative transfer, Zenodo [code], https://doi.org/doi.org/10.5281/zenodo.11234716, 2024.

Veerman, M. A., van Stratum, B. J., and van Heerwaarden, C. C.: A Case Study of Cumulus Convection Over Land in Cloud-Resolving Simulations With a Coupled Ray Tracer, Geophysical Research Letters, 49, e2022GL100 808, https://doi.org/10.1029/2022GL100808, 2022.

Wiltink, J. I., Deneke, H., van Heerwaarden, C. C., and Meirink, J. F.: Evaluating parallax and shadow correction methods for global horizontal irradiance retrievals from Meteosat SEVIRI, Atmospheric Measurement Techniques, 18, 3917–936, https://doi.org/10.5194/amt-18-3917-2025, 2025.

Zinner, T. and Mayer, B.: Remote sensing of stratocumulus clouds: Uncertainties and biases due to inhomogeneity, Journal of Geophysical Research: Atmospheres, 111, 14 209, https://doi.org/10.1029/2005JD006955, 2006.